Cell

SRD5A3 Is Required for Converting Polyprenol to Dolichol and Is Mutated in a Congenital Glycosylation Disorder

Vincent Cantagrel,[1] Dirk J. Lefeber,[2,3] Bobby G. Ng,[7] Ziqiang Guan,[8] Jennifer L. Silhavy,[1] Stephanie L. Bielas,[1] Ludwig Lehle,[9] Hans Hombauer,[10] Maciej Adamowicz,[11] Ewa Swiezewska,[13] Arjan P. De Brouwer,[4] Peter Blümel,[14] Jolanta Sykut-Cegielska,[12] Scott Houliston,[7] Dominika Swistun,[1] Bassam R. Ali,[15] William B. Dobyns,[17] Dusica Babovic-Vuksanovic,[18] Hans van Bokhoven,[4,5] Ron A. Wevers,[2] Christian R.H. Raetz,[8] Hudson H. Freeze,[7] Éva Morava,[6] Lihadh Al-Gazali,[15,16,*] and Joseph G. Gleeson[1,*]

[1]Neurogenetics Laboratory, Institute for Genomic Medicine, Howard Hughes Medical Institute, Department of Neurosciences and Pediatrics, University of California, San Diego, La Jolla, CA 92093, USA
[2]Department of Laboratory Medicine, Institute for Genetic and Metabolic Disease
[3]Department of Neurology
[4]Department of Human Genetics, Nijmegen Centre for Molecular Life Sciences
[5]Department of Cognitive Neuroscience, Donders Institute for Brain, Cognition, and Behaviour
[6]Department of Paediatrics, Institute for Genetic and Metabolic Disease
Radboud University Nijmegen Medical Centre, 6500 HB Nijmegen, The Netherlands
[7]Genetic Disease Program, Sanford Children's Health Research Center, Sanford-Burnham Medical Research Institute, La Jolla, CA 92037, USA
[8]Department of Biochemistry, Duke University Medical Center, Durham, NC 27710, USA
[9]Universität Regensburg, Lehrstuhl für Zellbiologie und Pflanzenbiochemie, D-93053 Regensburg, Germany
[10]Ludwig Institute for Cancer Research, Department of Medicine, Department of Cellular and Molecular Medicine and Cancer Center, University of California, San Diego, School of Medicine, La Jolla, CA 92093, USA
[11]Department of Biochemistry and Experimental Medicine
[12]Department of Metabolic Diseases, Endocrinology, and Diabetology
The Children's Memorial Health Institute, 04-730 Warsaw, Poland
[13]Institute of Biochemistry and Biophysics, Polish Academy of Sciences, 02-106 Warsaw, Poland
[14]Preyer'sches Kinderspital, 1100 Vienna, Austria
[15]Department of Pathology
[16]Department of Pediatrics
United Arab Emirates University, School of Medicine and Health Sciences, 17666 Al Ain, United Arab Emirates
[17]Department of Human Genetics, Neurology, and Pediatrics, University of Chicago, Chicago, IL 60637, USA
[18]Departments of Medical Genetics, Pediatric Neurology, Laboratory Genetics, Pediatric Endocrinology, and Dermatology, Mayo Clinic, Rochester, MN 55905, USA
*Correspondence: algazali@hotmail.com (L.A.-G.), jogleeson@ucsd.edu (J.G.G.)
DOI 10.1016/j.cell.2010.06.001

SUMMARY

N-linked glycosylation is the most frequent modification of secreted and membrane-bound proteins in eukaryotic cells, disruption of which is the basis of the congenital disorders of glycosylation (CDGs). We describe a new type of CDG caused by mutations in the *steroid 5α-reductase type 3* (*SRD5A3*) gene. Patients have mental retardation and ophthalmologic and cerebellar defects. We found that SRD5A3 is necessary for the reduction of the alpha-isoprene unit of polyprenols to form dolichols, required for synthesis of dolichol-linked monosaccharides, and the oligosaccharide precursor used for N-glycosylation. The presence of residual dolichol in cells depleted for this enzyme suggests the existence of an unexpected alternative pathway for dolichol de novo biosynthesis. Our results thus suggest that SRD5A3 is likely to be the long-sought polyprenol reductase and reveal the genetic basis of one of the earliest steps in protein N-linked glycosylation.

INTRODUCTION

N-glycosylation occurs on certain asparagine residues present on nascent polypeptides in all eukaryotic cells. The glycan structures resulting from this process show an incredible variability depending on the protein, cell type, and species. This essential posttranslational modification occurs on most secreted and plasma membrane proteins and is involved in protein folding and trafficking with implications for cell-cell and cell-matrix interactions and intracellular signaling (Freeze, 2006; Helenius and Aebi, 2001). The process of N-linked protein glycosylation is localized in the endoplasmic reticulum (ER) and the Golgi

compartment. Three separate phases can be distinguished: First, an oligosaccharide precursor, a block of 14 monosaccharides ($Glc_3Man_9GlcNAc_2$), is assembled on the lipid carrier dolichol-phosphate (Dol-P) in the ER membrane. Second, this glycan is transferred cotranslationally or posttranslationally to dedicated asparagine residues of nascent glycoproteins (Ruiz-Canada et al., 2009). In this reaction, oligosaccharyltransferase (OST) recognizes the acceptor sequence NX[S/T] (where X can be any amino acid except proline) on nascent polypeptides and catalyzes the transfer of the glycan precursor en bloc from its lipid carrier to the protein (Chavan and Lennarz, 2006). Third, the N-linked glycan is further modified by a series of trimming and elongation reactions beginning in the ER and ending in the late Golgi compartment.

The early steps of this pathway are present not only in eukaryotic cells but also in archae and bacteria, all relying on a lipid to build an oligosaccharide precursor (Jones et al., 2009). This carrier lipid, a polyisoprenoid, is assembled from a variable number of isoprene units, linked head to tail. The length of the carrier polyisoprenoid varies across evolution: bacteria posses a single predominant polyprenol, usually undecaprenol (composed of 11 isoprene units), but in eukaryotic cells these lipids typically occur as mixtures of different lengths, depending upon the species. In mammalian cells, dolichols are predominantly 18–21 isoprene units in length.

A requirement in eukaryotic organisms is the reduction of the precursor polyprenol to dolichol on the terminal isoprene unit (alpha) (Swiezewska and Danikiewicz, 2005), followed by phosphorylation to generate Dol-P. The identification of Dol-P as glycosyl carrier lipids in glycosylation was described 40 years ago (Behrens and Leloir, 1970), but the role of the free lipid, broadly distributed in mammalian cells (Rip et al., 1985), and some of its biosynthetic steps remain elusive. Using prenol labeling studies, a pathway for dolichol biosynthesis was proposed (Sagami et al., 1993); however, several enzymes were still missing, including a polyprenol reductase. In this article, the term ''polyprenol'' will be restricted to alpha-unsaturated compounds, despite its more general meaning, to distinguish them from dolichol, as it is commonly done in the literature. Several glycosylation-defective cell lines, generated in vitro, showed accumulation of polyprenol instead of dolichol (Acosta-Serrano et al., 2004; Rosenwald et al., 1993) and suggested that polyprenol reduction was the rate-limiting step in dolichol synthesis, with major consequences on N-glycosylation.

In humans, a disruption of N-glycosylation results in congenital disorders of glycosylation (CDGs), a growing class of hereditary disorders (Freeze, 2006; Grünewald and Matthijs, 2000; Haeuptle and Hennet, 2009; Jaeken and Matthijs, 2007). Defects in the maturation and transfer of the glycan precursor, located in the ER, have been grouped in the past as CDG type I, and disorders affecting the subsequent N-glycan processing steps grouped as CDG type II. A recently proposed alternate nomenclature uses only the gene name together with a CDG suffix (Jaeken et al., 2009). These diseases show wide symptomatology and severity. The main features are psychomotor retardation, cerebellar ataxia, seizures, retinopathy, liver fibrosis, coagulopathies, failure to thrive, and dysmorphic features including abnormal fat distribution and ophthalmological anomalies (Eklund and Freeze, 2006). Even though a multisystem phenotype is often observed, several cases have been reported with primary neurological involvement including cerebellar ataxia (Vermeer et al., 2007), suggesting that cerebellar disease maybe a sensitive measure of defective N-glycosylation.

In this study, we identify SRD5A3 orthologs as necessary for and promoting the reduction of polyprenol to dolichol in human, mouse, and yeast and describe a new syndrome of CDG type I in seven families caused by a defect in this newly identified polyprenol reductase.

RESULTS

Loss of Function Mutations of the *SRD5A3* Gene Cause a Multisystemic Syndrome with Eye Malformations, Cerebellar Vermis Hypoplasia, and Psychomotor Delay

We identified a large consanguineous Emirati family of Baluchi (Southern Iran) origin (CVH-385, Figure 1A) (Al-Gazali et al., 2008). All affected children displayed ocular colobomas, ichthyosis, heart defect, developmental delay, and brain malformations including cerebellar vermis hypoplasia. We performed a genome-wide linkage analysis and mapped the disease locus on chromosome 4q12 with a multipoint logarithm (base 10) of odds (LOD) score of 4.2 (Figure 1B). This mapping defined an interval of 53.8–57.4 MB (between the markers rs751266 and rs899631) encompassing 42 genes (based on NCBI genome browser, build 36 version 3) (Figure 1C), which were screened with a systematic mutational analysis of candidates with bidirectional sequencing. Analysis of the *steroid 5α-reductase 3* (*SRD5A3*) gene, coding for a 318 amino acid enzyme of unknown function, identified a molecular rearrangement with a homozygous 3 bp deletion and a 10 bp insertion resulting in a predicted stop codon at amino acid 96 (Figure 1D). To exclude the possibility that this change represented a common polymorphism, we tested 96 DNAs (192 chromosomes) from geographically matched controls but identified no carriers. Although CHIME syndrome (*c*olobomas of the eye, *h*eart defects, *i*chthyosiform dermatosis, *m*ental retardation, and *e*ar defects or *e*pilepsy) was the closest related disease without a known molecular cause (Sidbury and Paller, 2001), four families with this syndrome tested negative for *SRD5A3* mutations. However, another family of Baluchi origin (MR3) also living in the Emirates with a comparable phenotype (Table 1), displayed the same molecular rearrangement in *SRD5A3* (despite denying known relationship with CVH-385 family), suggesting the existence of a common founder mutation. Due to the phenotypic similarity with CDG, we tested the N-glycosylation status of transferrin using mass spectrometry (O'Brien et al., 2007), a reliable screening test for type I CDG patients. Transferrin is a serum protein with two N-glycosylation sites, fully occupied in control individuals. CVH-385 and MR3 patients showed a very clear defect with, respectively, about 45% and 25% of monoglycosylated transferrin, suggesting that the *SRD5A3* mutation leads to a type I CDG (Figure 2A and Figure S2A available online). We also found a defect in extra-cellular secretion of N-glycosylated DNase I in index patients' fibroblasts (Figure S2B), a sensitive measure of defective N-glycosylation (Nishikawa and Mizuno, 2001; Vleugels et al., 2009).

Consequently, we screened 38 patients with CDG type I-x (CDG type I negative for known gene mutations), and we identified five other independent homozygous or compound heterozygous mutations and one genomic rearrangement (Figure 1F, Table 1, and Figure S1). Among the mutations identified were a 2 bp deletion and four single-base substitutions resulting in stop codons. Additionally, patient AK0295 carried a homozygous truncation of the gene encompassing within exon 5, in the 3′ part of *SRD5A3* open reading frame (ORF). Further expression analysis in patients' fibroblasts showed partial nonsense-mediated messenger RNA (mRNA) decay of *SRD5A3* transcript in some patients (Figure 1G).

Based on the phenotype of 11 children from seven families, the most striking features observed were the presence of congenital eye malformations with variable degree of visual loss, nystagmus, muscle hypotonia, motor delay, mental retardation, and facial dysmorphism. Microcytic anemia, elevated levels of liver enzyme activities, coagulation abnormalities, and decreased antithrombin III levels were detected in nine evaluated cases. Most children presented with ocular coloboma or hypoplasia of the optic disc (unique features in the CDGs) (Morava et al., 2009), with striking cerebellar atrophy or vermis malformation. Ichthyosiform erythroderma or dry skin and congenital heart malformations were sporadically present. Midline malformations and endocrine anomalies were only present in the index patients (Al-Gazali et al., 2008) (Table 1). The relative uniformity in the biochemical and clinical phenotype associated with frequent early truncating mutations suggests loss-of-function of *SRD5A3* as the genetic mechanism.

Patients with Mutation in *SRD5A3* Show an Early Defect in Lipid-Linked Oligosaccharide Synthesis

The absence of whole glycan chains on proteins indicated that the metabolic block occurred early in the N-glycosylation pathway, altering synthesis or transfer of the glycan part of lipid linked oligosaccharide (LLO), to recipient proteins. Epitope tagged SRD5A3 localized predominantly to the ER (Figure 2B), where LLO synthesis occurrs (Aebi and Hennet, 2001).

An abnormal composition of the glycan precursor impairs its transfer to acceptor proteins. Accordingly, we investigated the size of the LLO glycans using HPLC after [2-^{3}H]-mannose metabolic labeling with fibroblasts from index patients CVH-385-IV-11 and CVH-385-IV-13. Since no major structural abnormalities in LLO were detected (Figure S2E), we also determined the amount of radiolabeled LLO. We detected a severe reduction in the amount of newly synthesized LLO in four of the five patients tested compared to three control cell lines (Figure 2C), suggesting that the N-glycosylation block occurs prior the glycan transfer step.

The reduced levels of LLO could be explained by a limited availability of Dol-P. To test this hypothesis, we used an in vitro assay to assess the production of Dol-PP-GlcNAc$_1$ and Dol-PP-GlcNAc$_2$, the first two reactions of LLO synthesis. With fibroblast homogenates used as a source of enzyme and UDP-[^{14}C]GlcNAc as glycosyl donor, all *SRD5A3* deficient patient samples showed a reduced synthesis of Dol-PP-GlcNAc$_{1/2}$ without addition of exogenous Dol-P, compared to controls (Figure 2D). However, when exogenous Dol-P was added to the incubation mixture, formation of Dol-PP-GlcNAc$_{1/2}$ was increased to levels comparable with or even higher than controls. Fibroblasts from patients with other known CDG-I defects (CDG-Ik or CDG-Io) behaved comparable to controls, showing no evidence of Dol-P mediated rescue (Figure 2D). Elongation of Dol-PP-GlcNAc$_2$ to Dol-PP-GlcNAc$_2$-Man$_5$ was unremarkable. Similarly, OST activity was normal (data not shown). Altogether, the rescue of the enzymatic GlcNAc transferases deficiencies by exogenous Dol-P indicates that the amount of Dol-P is limiting in the patients' fibroblasts and suggests a defect in Dol or Dol-P biosynthesis.

SRD5A3 Is the Human Ortholog of the Yeast *DFG10/YIL049W* Gene

A yeast mutant for the *DFG10* gene, called *dfg10-100*, was previously isolated by a genetic screen for mutant strains *d*efective for *f*ilamentous *g*rowth (dfg), using insertional mutagenesis (Mösch and Fink, 1997). The product of this gene shows 25% amino acid identity and 43% similarity with the human SRD5A3 protein (Blastp, NCBI). To determine whether *DFG10* is the yeast ortholog of *SRD5A3* (Figure 3A), we first asked whether the *dfg10-100* mutant displays a lack of N-glycan modifications. Carboxypeptidase Y (CPY) is a secreted enzyme with a mature form that contains four N-glycan sites, all of which are occupied under optimal growth conditions (Hasilik and Tanner, 1978) and all of which can be removed with PNGase F treatment. In contrast with the WT strain (L5366), the *dfg10-100* mutants (diploid and homozygous at the *DFG10* locus) produced hypoglycosylated CPY, with the detection of tri-, di- and monoglycosylated CPY (Figure 3B). Because the *dfg10-100* mutant is a result of a transposon insertion into the *DFG10* promoter, it was possible that still some protein was expressed, thus accounting for the nonlethal phenotype. This possibility was excluded by engineering a deletion of the whole *DFG10* ORF, which produced an identical growth delay and CPY phenotype (Figure S3). The identification of a similar biochemical defect in yeast and human suggests a conserved function for *SRD5A3* across evolution.

In human, five partially homologous genes compose the steroid 5α-reductase family, including the well-characterized *SRD5A1*, *SRD5A2* involved in testosterone reduction (Russell and Wilson, 1994), encoding for proteins targeted in treatments against prostatic hyperplasia and male pattern hair loss (Aggarwal et al., 2010), and also *SRD5A2L2*, *GPSN2*, *SRD5A3* that are less characterized. Bioinformatics comparison showed that the DFG10 sequence shares most identity with SRD5A3 (BLASTP, E value = 2e-13) whereas SRD5A1, SRD5A2, SRD5A2L2 and GPSN2 show E values of, respectively 6e-04, 3e-04, 3e-04 and 5e-05 (Figure 3A). To test for functional conservations we expressed each mammalian ORF under the control of a strong constitutive yeast promoter (Alber and Kawasaki, 1982) in the *dfg10-100* mutant. The mutant transformed with yeast *DFG10* showed a full correction of the CPY underglycosylation. Furthermore, *SRD5A3* was the only homolog able to rescue the phenotype (Figure 3C). This experiment shows that *SRD5A3* is the diverged human ortholog of the yeast *DFG10* gene and suggests a specific role for *SRD5A3* in protein glycosylation compared with other family members.

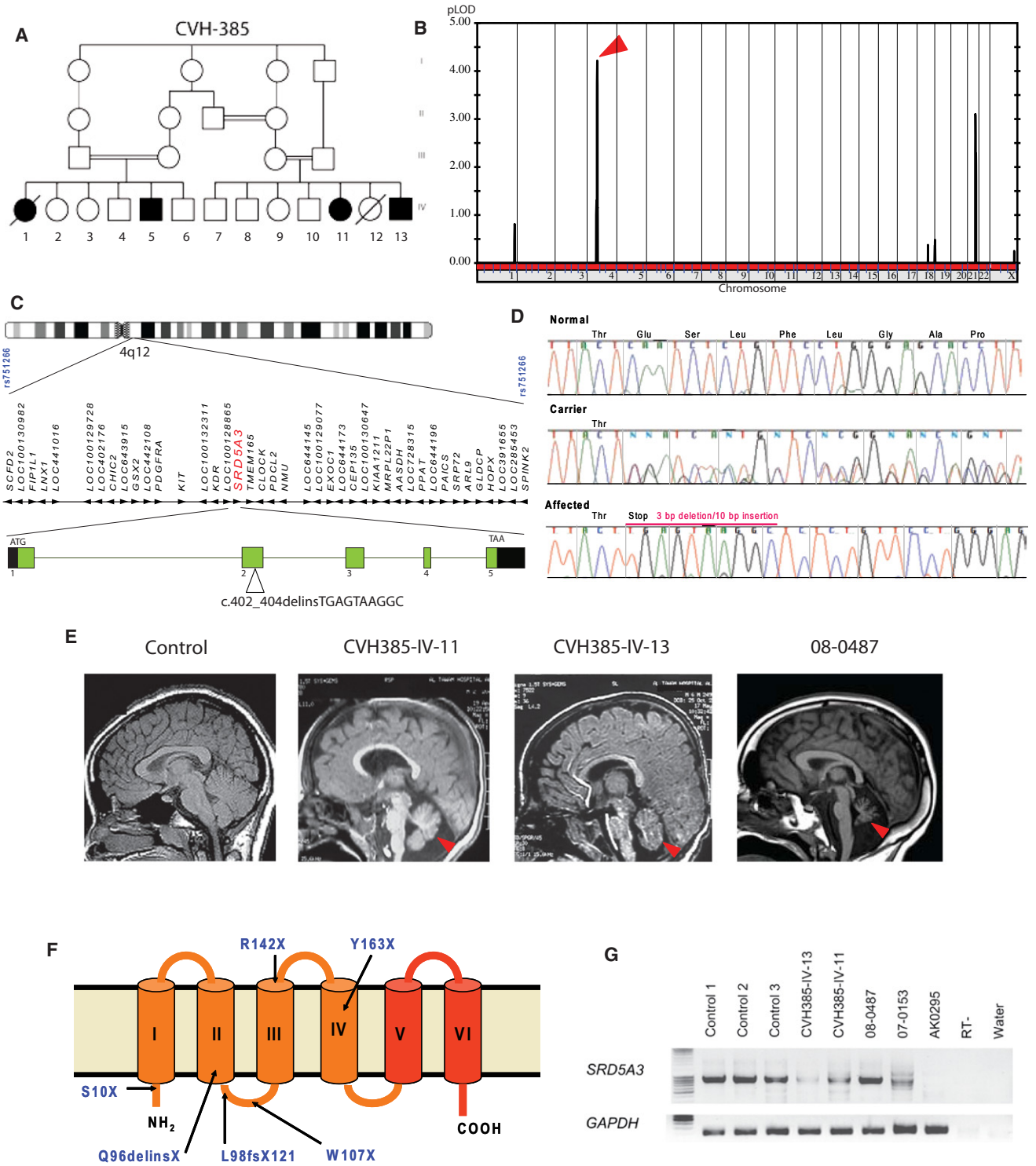

Figure 1. Identification of Mutations in the *SRD5A3* Gene in Patients with Multisystemic Syndrome Including Cerebellar Hypoplasia

(A) Pedigree of family CVH-385 showing several levels of consanguinity with cousin marriages. The two branches each produced two affected offspring represented by filled symbols in generation IV.

(B) Whole-genome analysis of linkage results with chromosomal position (x axis) and multipoint LOD score (y axis) showing a peak LOD score of 4.2 on chromosome 4 (arrowhead).

(C) Expanded view of the candidate interval on chromosome 4q12, containing 42 candidate genes including *SRD5A3* (red), spanning 25.5 kb of genomic DNA with 5 exons. A mutation in exon 2 was identified in family CVH-385.

Table 1. Clinical Phenotype Associated with *SRD5A3* Mutations

	CVH-385	MR3	08-0487/86	08-0904	07-0153	07-0419	AK0295
Ethnic background	Baluchi	Baluchi	Polish	Turkish	Polish	Turkish	Iranian
Consanguinity	+	+	+	+	−	+	+
Muscle hypotonia/motor retardation	+/−	+	+	+	+	+	+
Mental retardation	+	+	+	+	+	+/−	+
Cerebellar atrophy/ vermis malformations	+	NA	+	+	+	−	+
Spasticity	+/−	+/−	+	−	−	−	−
Movement disorder/dystonia	−	+/−	+	−	−	−	+/−
Visual loss	+/−	+	+	+	+	+/−	+
Hypoplasia or coloboma/ iris/retina/chorioid/optic disc	+	+	+	+	+	−	+
Nystagmus	+	+	+	+	+	+	+
Optic atrophy	+	+	+	+	+	−	−
Other eye malformation (microphthalmia / glaucoma/cataract)	microphthalmia	−	+	cataract	−	glaucoma	microphthalmia cataract
Cardiac malformation/ cardiac hypertrophy	+	−	−	−	−	−	−
Ichtiosis/erythroderma	+	−	−	+	+	−	+
Dry skin/atopic dermatitis	+	+	+/−	−	+	−	+
Inverted nipples	−	−	−	+	−	+	−
Joint contractures	+/−	−	−	−	−	−	−
Swallowing problems	+	+	−	−	−	−	+
Failure to thrive	+	−	−	−	−	−	+
Microcytic anemia	+	+	+	+	−	−	+
Elevated liver enzymes	+	NA	+	+	+	+	+
Abnormal coagulation studies	NA	NA	+	+	+	+	+
Decreased antithrombine 3/protein C and S levels	NA	NA	+	+	+	+	+
Mutation cDNA	c.286_288 delins TGAGTAAGGC	c.286_288 delins TGAGTAAGGC	c.292_293 del	c.320 G→A	het c.424 C→T het c.489 C→A	c.29 C→A	Genomic rearrangement
Mutation at protein level	p.Gln96 delinsX	p.Gln96 delinsX	p.Leu98 ValfsX121	p.Trp107X	p.Arg142X p.Tyr163X	p.Ser10X	Absent

NA, data not available.

Phylogenetic analysis of proteins with a steroid 5α-reductase domain from multiple species indicates that this steroid reductase family can be separated in three main groups consisting of (1) the SRD5A1-SRD5A2 group, (2) the SRD5A3 group containing DFG10, and (3) the GPSN2-SRD5A2L2 group (Figure S3), supporting the idea that different classes of lipids can be substrates for these enzymes and suggesting that the substrate of the enzyme encoded by the common ancestral gene was potentially not a steroid.

(D) DNA sequence of exon 2 of *SRD5A3* from a control individual, an obligate carrier, and an affected family member from CVH-385. The mutation consists of a 3 bp deletion associated with a 10 bp insertion, resulting in a frame shift and premature termination at amino acid 96 of 318, within the second of six transmembrane domains.

(E) Brain MRI midline sagittal view showing cerebellar vermis hypoplasia (red arrowhead) in *SRD5A3* mutated patients.

(F) Topology model of SRD5A3 with mutations indicated and six transmembrane domains. Mutations were scattered throughout the ORF, all leading to predicted protein termination before the steroid reductase domain (in red).

(G) Amplification of the *SRD5A3* transcript by RT-PCR with RNA extracted from controls and patient fibroblasts. The expression level of the gene is lower in almost all patients CVH-385-IV-13, CVH-385-IV-11, 07-0153 compared to control, suggesting nonsense-mediated mRNA decay. No expression was detected in patient AK0295, as a result of a homozygous genomic rearrangement. RT−, no reverse transcriptase; water, no cDNA.

See also Figure S1.

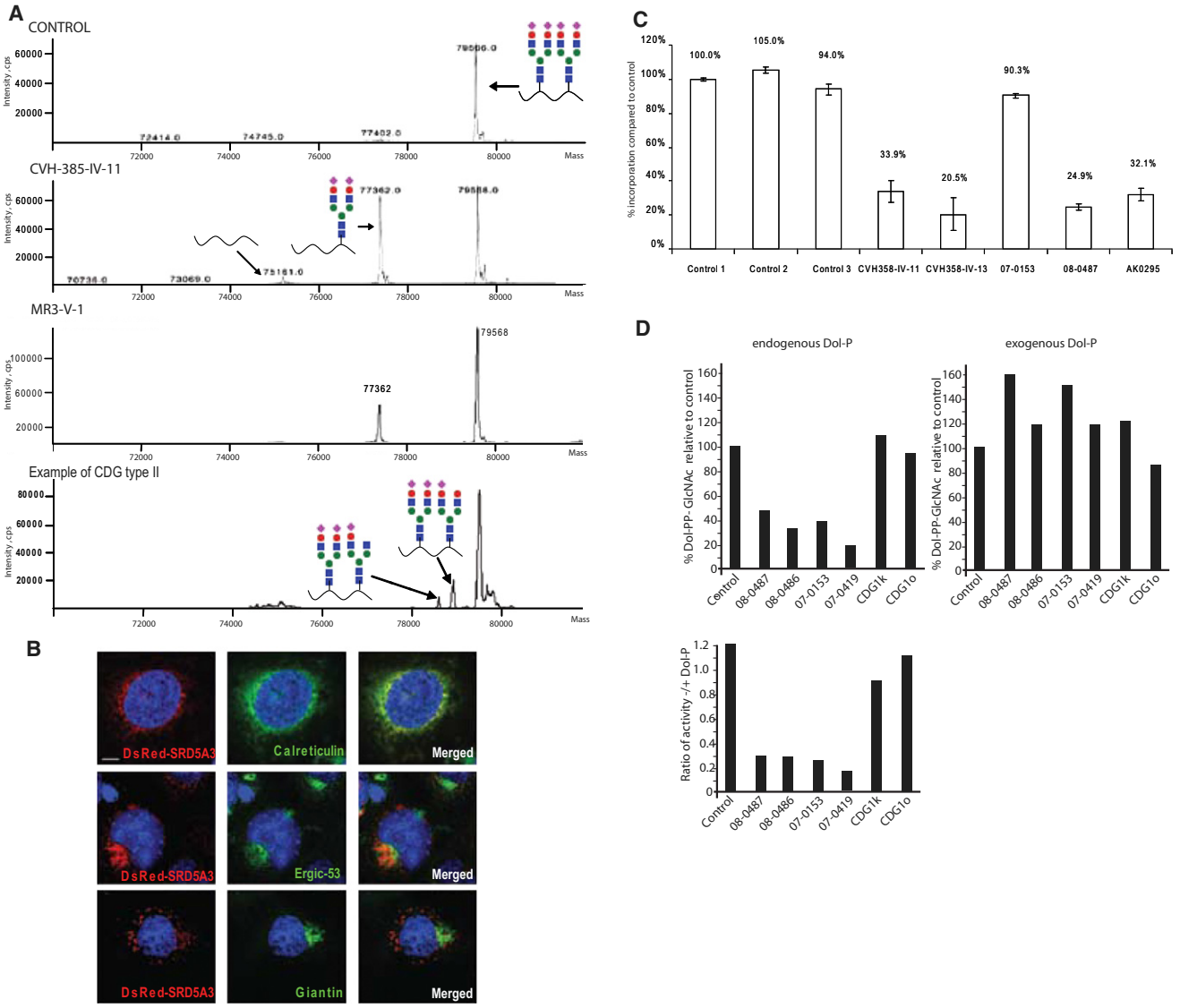

Figure 2. *SRD5A3* Mutated Patients Have a Congenital Disorder of Glycosylation Type I Caused by a Defect in LLO Synthesis, Rescued In Vitro with Exogenous Dolichol Phosphate

(A) Mass spectra of transferrin, normally N-glycosylated on two sites, Asn-432 and Asn-630 (control). Transferrin containing a single N-glycan in *SRD5A3* patient samples was increased, indicating a CDG type I disorder. An example of transferrin profile from CDG type II patient, with two glycan chains but abnormal structure (depicted by lack of certain sugar moieties), is shown for comparison.

(B) Intracellular localization of SRD5A3 containing a N terminus DsRed tag (center panel) in COS7 cells costained with antibody against ER-specific marker, calreticulin, ERGIC-specific marker ERGIC53, and Golgi-specific marker Giantin. DsRed-SRD5A3 colocalized with most of the ER whereas Giantin staining did not colocalize. The scale bar represents 10μm.

(C) Incorporation of [^{3}H]-mannose into LLO after labeling of human fibroblasts. The results indicate severely reduced levels of LLO in four out of five patient samples. Error bars represent the mean ± standard deviation from three experiments.

(D) Rescue of LLO precursor levels with exogenous Dol-P. GlcNAc transferase activity in fibroblasts was measured. Microsomal fractions from fibroblasts were incubated with radioactive GlcNAc, and then Dol-PP-GlcNAc$_{1/2}$ formation was analyzed by TLC. Extracts from patients' fibroblasts produced a reduced amount of Dol-PP-GlcNAc$_{1/2}$. However, the addition of exogenous Dol-P rescued this defect.

See also Figure S2.

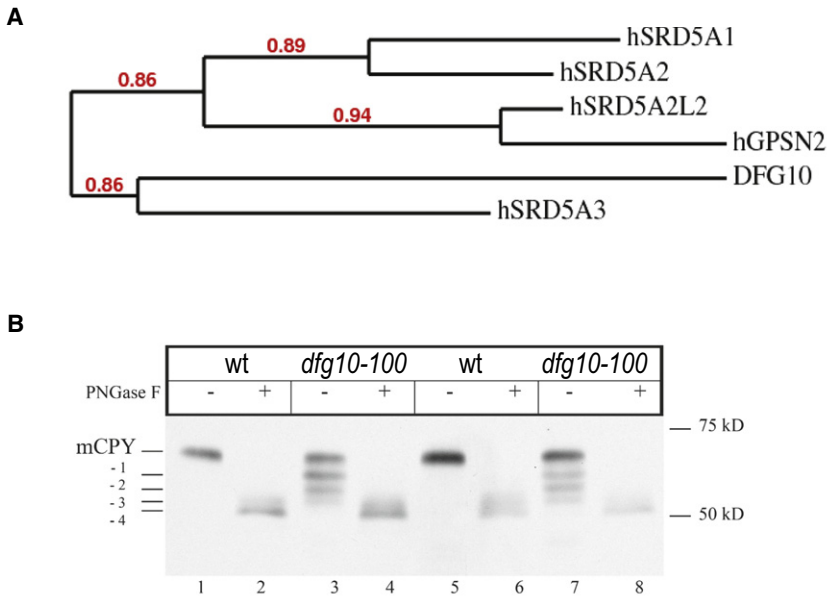

Figure 3. N-Glycosylation Phenotype of *dfg10-100* Yeast Mutant and Rescue with Human *SRD5A3*

(A) Phylogenic tree representation of the yeast protein DFG10 and human proteins presenting a steroid 5α-reductase domain, with branch support value indicated in red.

(B) N-glycosylation status of the yeast protein CPY in yeast WT and *dfg10-100* mutant strain, mutated by transposon insertion. Two colonies from each strain were tested. CPY is posttranslationally modified by the addition of four glycan chains. In the *dfg10-100* mutants, a protein lacking one, two, or three glycan chains is detected. Protein extracts were treated with PNGase F to remove the N-glycans.

(C) Glycosylation status of CPY in *dfg10-100* mutant transformed with each steroid 5α-reductase domain containing gene from human. Only *SRD5A3* showed rescue effect. Positions of mature CPY (mCPY) and the different glycoforms (−1, −2, −3, −4) are indicated. Vector indicates empty vector control.

See also Figure S3.

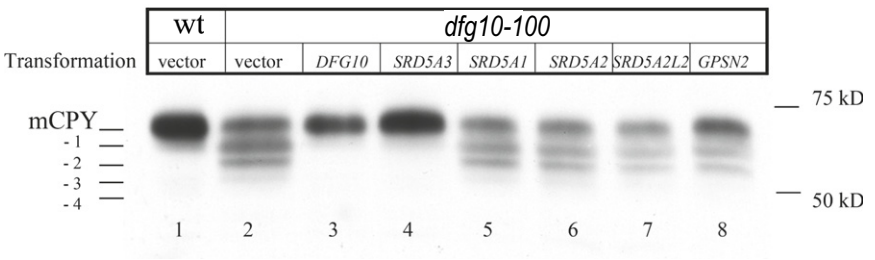

Srd5a3 Mutation Is Lethal in Mouse and Results in an Activation of the Unfolded Protein Response Pathway

We found that mice homozygous for a LacZ gene trap (Gt) insertion in intron 3 of *Srd5a3* were recovered at embryonic stages, up to embryonic day 12.5 (E12.5) but not beyond (Figures 4A and 4B). At E10.5, *Srd5a3*$^{Gt(betaGeo)703Lex/Gt(betaGeo)703Lex}$ embryos (abbreviated *Srd5a3*$^{Gt/Gt}$) were smaller and failed to undergo axial rotation observed at E8.5 in WT littermates. Analysis with β-gal colorimetric staining in asymptomatic heterozygous carriers showed strong expression in the yolk sac, eyes, heart, and neural tube (Figures S4A–S4D). In keeping with this, homozygous mutants frequently presented dilated hearts (Figure 4A) and open neural tubes, which is consistent with the broad phenotypes observed in patients.

To identify the misregulated pathways underlying these developmental defects, we carried out expression microarray analysis in *Srd5a3*$^{Gt/Gt}$ embryos versus WT littermates before morphological differences appeared (Figure 4C). Whole-transcriptome analysis revealed that among the 50 most upregulated transcripts, 20% are involved in the regulation of the unfolded protein response (UPR) or are activated in this pathway (Tables S1 and S2). An activation of the UPR pathway in E8.5 *Srd5a3*$^{Gt/Gt}$ embryos was confirmed by real-time RT-PCR and with an E9.5 mouse embryonic fibroblast cell line treated with tunicamycin used as a positive control (activates the UPR pathway by blocking N-glycosylation; Figure 4D). A marker of this pathway, BiP, is upregulated at the transcript and protein levels in *Srd5a3*$^{Gt/Gt}$ embryos, with a particularly high expression in neuroepithelial cells (Figure 4E). *Srd5a3* expression was not detected in mutant embryos; however, in cells inhibited for N-glycosylation by tunicamycin treatment, its expression increased significantly (Figure 4D). We also confirmed UPR activation by determining enrichment of gene ontology (GO) categories by all the genes significantly misregulated in *Srd5a3*$^{Gt/Gt}$ embryos compared with littermate controls. UPR was the biological process most significantly enriched for the genes upregulated (Table S3), whereas genes involved in general cellular metabolic processes and specific embryonic developmental program like regionalization were the most significantly downregulated (Table S3). These observations suggest that *Srd5a3* is required for ER protein folding, a primary role of N-glycan during development.

DFG10 and *SRD5A3* Are Necessary for Conversion of Polyprenol to Dolichol in Yeast, Mouse, and Human

During the de novo synthesis of dolichol in eukaryotes, the farnesyl pyrophosphate (FPP), a product of the mevalonate pathway, is elongated by its successive condensation with isopentenyl pyrophosphate (IPP), catalyzed by a *cis*-isopentenyltransferase named dehydrodolichyl diphosphate synthase (DHDD) (Figure 5A). According to the current model, when the chain reaches target length, the pyrophosphate and phosphate groups are removed, although the phosphatases are not yet identified (Kato et al., 1980; Wolf et al., 1991). The alpha-isoprene unit of polyprenol is subsequently reduced by an NADPH-dependent

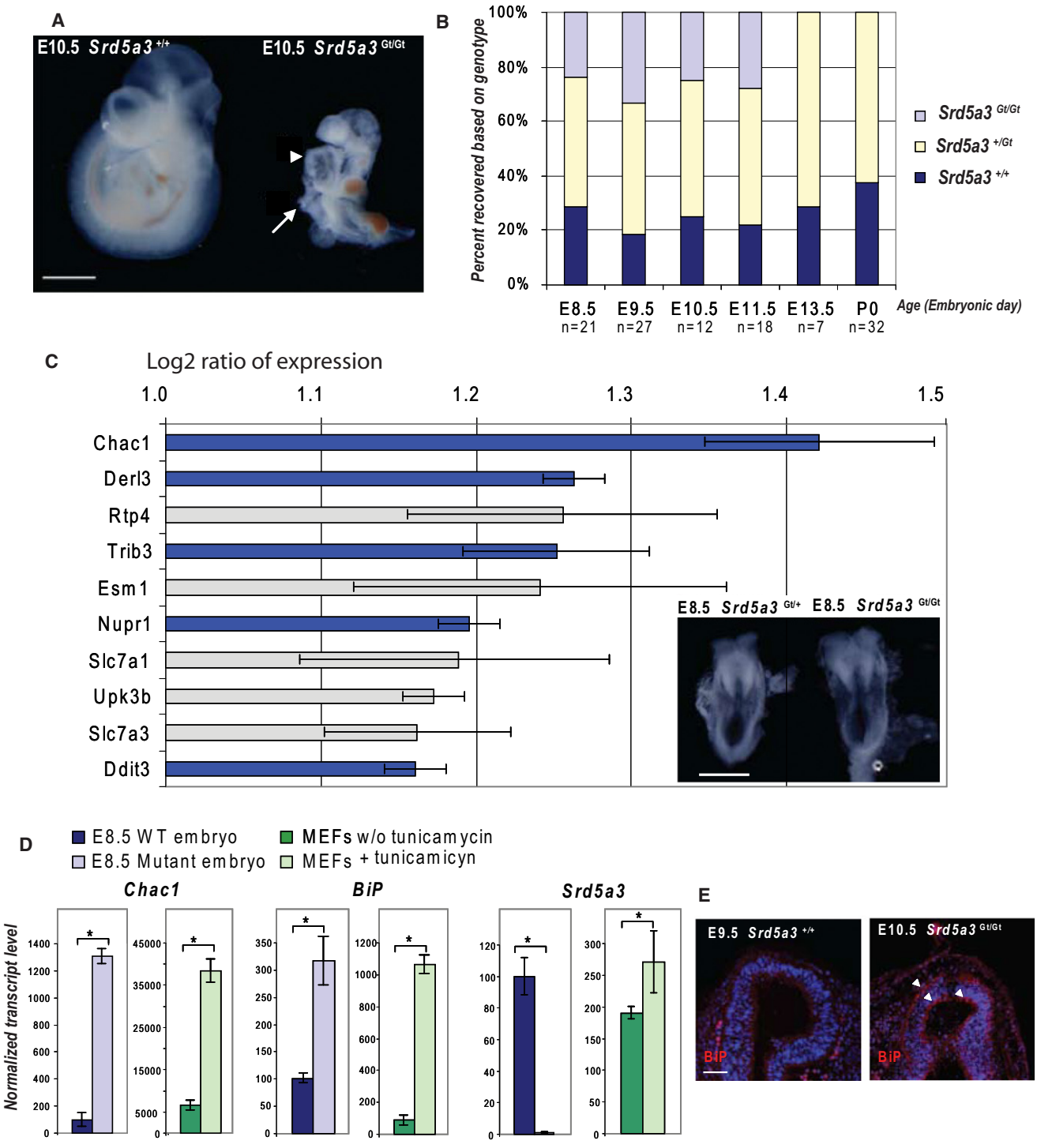

Figure 4. Characterization of Homozygous *Srd5a3*$^{Gt/Gt}$ Gene Trap Mouse Embryos

(A) Phenotype at E10.5 shows failure to rotate, ventral body wall defect (arrow), and dilated heart (arrowhead). The scale bar represents 1 mm.

(B) Graphic representation of the genotype obtained from the progeny of heterozygous mating, with lethality appearing between E11.5 and E13.5.

(C) Genes overexpressed in *Srd5a3*$^{Gt/Gt}$ at E8.5 detected with 44k mouse genome oligo microarray (1 is the log 2 of a 2-fold expression increase; error bars represent the mean ± standard deviation from four independent experiments). Among ten of the most upregulated genes, five (in blue) are involved in the unfolded protein response pathway (UPR). Morphology of heterozygous and homozygous *Srd5a3* mutant embryos at E8.5, before embryo axial rotation. The scale bar represents 500 μm.

(D) Real-time RT-PCR confirming activation of the UPR pathway (Errors bars are means ± standard deviations, asterisks indicate $p < 0.05$, $n = 3$).

microsomal reductase (Sagami et al., 1993), but the enzyme involved has not been identified. Finally, a dolichol kinase (hDK), mutated in CDG-Im, transfers phosphate from CTP to dolichol (Allen et al., 1978; Kranz et al., 2007). The unidentified polyprenol reductase enzyme made SRD5A3 a likely candidate for this function.

To explore a disruption of the final step of dolichol biosynthesis in *SRD5A3* or *DFG10* mutated cells and to unequivocally identify the last step of dolichol synthesis, we used liquid chromatography-mass spectrometry (LC-MS) (Garrett et al., 2007) to analyze polyprenols in WT and *dfg10-100* yeast strains, E11.5 WT and *Srd5a3*$^{Gt/Gt}$ mouse embryos, and fibroblasts and leukocytes from controls and patients. Polyprenol was not detected in any samples of WT origin as reported (Swiezewska and Danikiewicz, 2005) but was easily detected in the yeast and mouse mutants, in the same molar range as the dolichol naturally present in control samples (Figures 5B and 5C), suggesting a block in the polyprenol reduction step. In reference to an internal standard, by correcting polyprenol isotopic contribution, we detected a 70% decrease in dolichol in the *dfg10-100* mutant compared to the WT yeast from the same background (Figure 5B, right end). Given these striking results in both mouse and yeast, we were surprised to find no clear change in prenol profiles in patient fibroblasts or leukocytes (data not shown). Because one possible explanation might be that the normal exogenous fetal calf serum used in tissue culture supplied dolichol to overcome this metabolic block, we instead analyzed directly patient fresh plasma. We found an increased level of polyprenoids in patients' samples versus controls and in other CDG-I patients with a significant increased of polyprenols-18,19,20/dolichols-18,19,20 ratios (Figure 5D), indicating a defect in polyprenols metabolism in all organisms tested.

SRD5A3 Promotes the Reduction of Polyprenol to Dolichol

We next tested whether SRD5A3 was capable of reducing polyprenol to dolichol. We assessed polyisoprenoid levels in yeast transformed with vectors expressing the human and the yeast enzymes (Figures 6A–6E), cultured in minimal media and harvested during the log phase. The important accumulation of polyprenol detected in the *dfg10-100 strain* (Figure 6B) is efficiently and specifically corrected in yeast transformed with the *SRD5A3* gene (Figure 6D) compared to other human steroid 5α-reductases (Figure S5), whereas a mutant *SRD5A3* (H296G) encoding an enzyme predicted to be inactive (Wigley et al., 1994) did not show any reduction of the accumulated polyprenol (Figure 6E). To evaluate whether SRD5A3 was able to facilitate polyprenol reduction, we used lysates of transfected HEK293T cells overexpressing tagged SRD5A3. Exogenous polyprenol-18 was added in a buffer containing different detergents and mixed with lysates containing NADPH (Figures 6F–6H′). Some exogenous polyprenol-18 was elongated to polyprenol-19, indicating a good incorporation of this lipid in the protein-lipid complexes from the lysate. The most efficient in vitro reduction was obtained with 0.1% Triton X-100; the reduction efficiency by the lysate of transfected cells with an empty vector was comparable with the previously described assay (Sagami et al., 1993). In control HEK293T cells, we found ~28% exogenous polyprenol reduced to dolichol, whereas in lysates overexpressing WT SRD5A3, we found ~67% reduction, (Figures 6F–6H′ and Figure S6E). These results suggest that transfected SRD5A3 promotes efficient reduction of polyprenol.

DISCUSSION

Biological Activity of SRD5A3

SRD5A3 sequence predicts a steroid 5α-reductase domain, and some enzymes with this domain are able to reduce a variety of steroid hormones with a delta4,5,3-oxo structure (Russell and Wilson, 1994). Mutation of the *SRD5A2* gene in human causes male pseudohermaphroditism as a result of an enzymatic block of testosterone to dihydrotestosterone conversion (Andersson et al., 1991), and mutation of the *Srd5a1* gene in mice affects reproduction and parturition, suggesting involvement in androgen metabolism (Mahendroo and Russell, 1999). Interestingly, a previous study suggested that cell extract containing overexpressed SRD5A3 was able to reduce testosterone to dihydrotestosterone (Uemura et al., 2008), albeit at a slow rate.

However, both our biochemical and clinical investigations in the patients with *SRD5A3* mutations indicate that the nature of the substrate of the SRD5A3 enzyme is not related to the steroids. Our patients displayed no abnormal sexual abnormalities that would have suggested a primary defect of steroid metabolism. Moreover, karyotype analysis excluded the possibility of sex reversal in all (data not shown). These observations lead us to hypothesize that the in vivo substrate of SRD5A3 could be a different lipid. Polyprenols share a common origin with cholesterol because they are also built from isoprene units.

Another enzyme with a predicted steroid 5α-reductase domain, Tsc13/GPSN2, has been shown to be an enoyl reductase involved in the elongation of very long chain fatty acids (Kohlwein et al., 2001). This study also illustrates that the predicted steroid 5α-reductase domain is involved in the reduction of a nonsteroid lipid and suggests that the full spectrum of lipid reduction mediated by steroid 5α-reductase-like enzymes needs further evaluation.

Current Models for Dolichol Biosynthesis

Several mechanisms have been proposed for the last steps of dolichol biosynthesis. One postulated an initial dephosphorylation of polyprenol diphosphate followed by reduction to Dol-P, then dephosphorylation of Dol-P to produce dolichol (Chojnacki and Dallner, 1988). However, several studies demonstrated the phosphorylation of dolichol as the major pathway for the production of Dol-P (Heller et al., 1992; Rossignol et al., 1983). A second proposal suggested that the final condensation reaction of Pol-PP uses isopentenol instead of isopentenyl-PP. In this reaction, Pol-PP is directly transformed to a one isoprene unit longer

(E) Immunofluorescence staining showing expression of BiP protein (red), a marker of the UPR pathway activation, in the neuroepithelium of the forebrain vesicle (arrowheads). The scale bar represents 50 μm.
See also Figure S4.

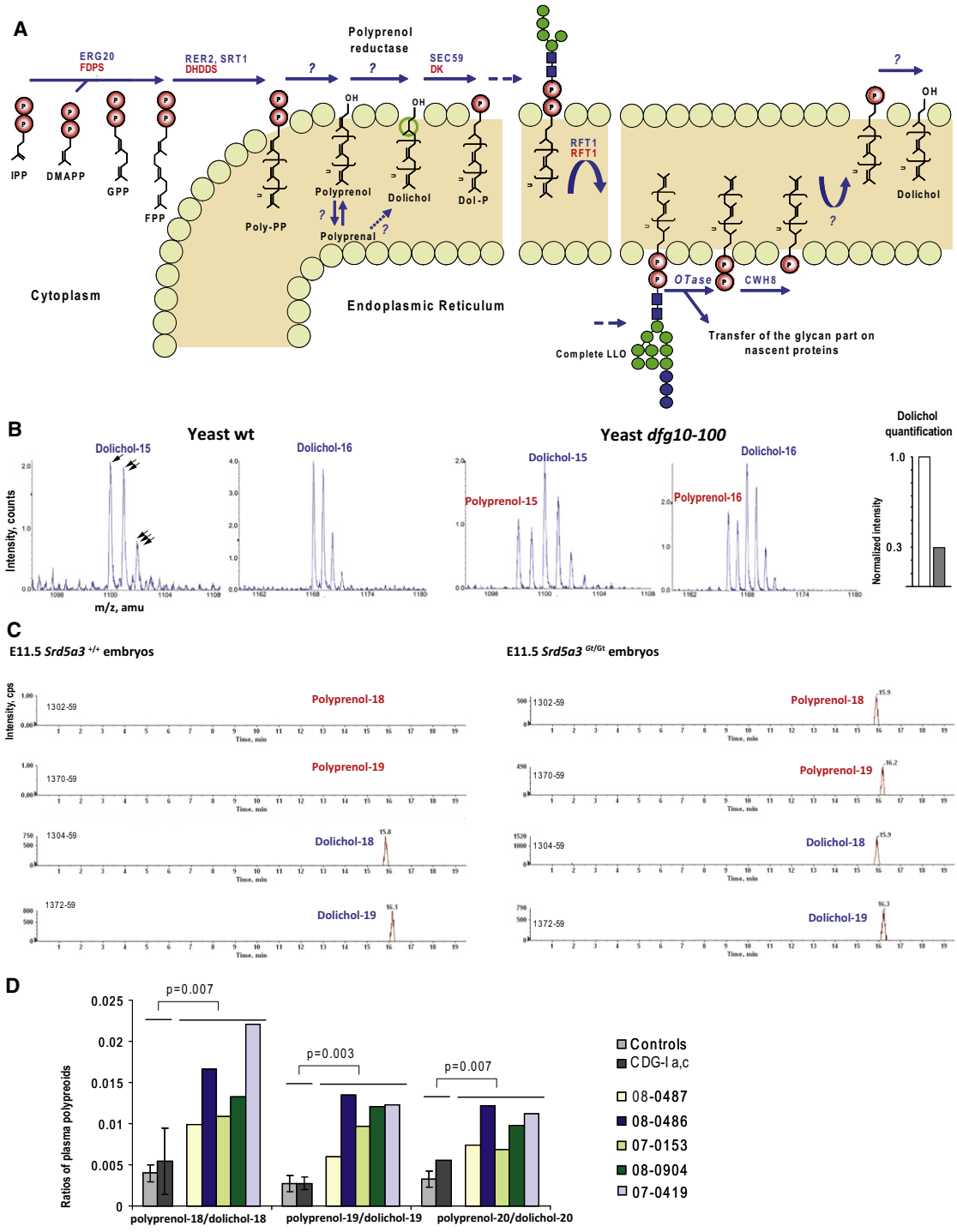

Figure 5. Analysis of Polyprenols and Dolichols, in Yeast, Mouse, and Human with LC-MS

(A) De novo biosynthesis and recycling of dolichol in eukaryotic cells with the yeast (in blue) and human (in red) enzymes involved. Isopentenylpyrophosphate (IPP) is the building block for all polyprenoids. IPP molecules are added sequentially in *trans*-configuration on dimethylallyl pyrophosphate (DMAPP) via the farnesyl pyrophosphate synthase (ERG20/FDPS) to form geranyl pyrophosphate (GPP) and then farnesyl pyrophosphate (FPP). More IPP units are then added in *cis*-configuration on FPP by the *cis*-prenyl transferases (RER2, SRT1/DHDDS), producing long polyprenoids that are embedded in the ER membrane. Once the final length is reached, both phosphate residues are released by unidentified phosphatases. The alpha-isoprene unit of the polyprenol is subsequently reduced by an NADPH-dependent microsomal reductase. For this step, the corresponding aldehydes have also been suggested as intermediates (Sagami et al., 1996). Finally the dolichol-specific kinase (SEC59/DK) transfers a phosphate from CTP to dolichol. Dol-P is used to build the lipid linked oligosaccharide (LLO). Once the oligosaccharide structure is transferred to specific asparagine residues, Dol-P is released on the luminal leaflet of the ER and is dephosphorylated by a pyrophosphatase (CWH8).

dolichol, thus circumventing the dephosphorylation steps (Ekström et al., 1987). The third proposal is the most widely accepted (Figure 5A) based on the finding of high concentrations of polyprenol during the initial phase of dolichol biosynthesis (Ekström et al., 1984) and the detection of a basal polyprenol reductase activity, in vitro (Sagami et al., 1993). However, the reductase postulated in this reaction had not been identified, and thus these models could not be directly evaluated. Our results suggest that SRD5A3 is the polyprenol reductase, which is consistent with the last model, confirming that the reduction of polyprenol is the major pathway for dolichol biosynthesis.

Residual Dolichol in *SRD5A3* Mutants

Dolichol was still detected in human, mouse, and yeast *SRD5A3/DFG10* mutants, suggesting the existence of another de novo biosynthetic pathway for dolichol production. The presence of dolichol in these mutants is not explained by dietary contribution, which was reported to be negligible in rat (Keller et al., 1982), and the nature of the mutations in human, mouse, and yeast suggests that these organisms have null mutations for this gene. These observations indicate the existence of an alternative pathway for de novo synthesis of dolichol in eukaryotic cells. Disruption of LLO biosynthesis due to mutation in *Dpagt1* in mouse results in embryonic lethality at E5 (Marek et al., 1999), a more severe phenotype than that observed in *Srd5a3* mutant mouse embryos, consistent with an alternative pathway. One candidate is the *TSC13* gene, the only other gene in *S. cerevisiae* encoding a steroid 5α-reductase domain (Pfam database). We tested whether the *tsc13* mutant had abnormal CPY glycosylation and whether the *dfg10/tsc13* double mutant showed further increase of the polyprenol/dolichol ratio, but found no effect of either (Figure S3), suggesting that the alternative pathway for dolichol synthesis is independent of these genes. Interestingly, among the pathways activated in embryonic mouse mutants was the mevalonate pathway, including the isoprenoid biosynthetic enzymes (Tables S1 and S2). This could suggest a positive feedback mechanism, which might help organisms overcome a partial block of these pathways.

Phenotypic Spectrum Resulting from Disruption of Dolichol Metabolism

Tissues affected in patients with *SRD5A3* mutations, such as nervous system, ocular structures, skin, or coagulation factors, reflect sensitivity for alteration in N-glycosylation. Such congenital defects and the detection of a restricted expression pattern of *Srd5a3* in mouse embryo suggest a spatial-temporal requirement during development. N-glycan number and branching regulate surface glycoprotein levels, affecting cell proliferation and differentiation (Lau et al., 2007). N-glycosylation may help regulate specific developmental pathways yet to be discovered. A comparable multisystem disorder has been recently mapped to the same locus, suggesting that these patients have the same genetic defect (Kahrizi et al., 2009).

Although we find defects in the N-glycosylation pathway, dolichol is also required for the synthesis of O-mannose-linked glycans, C-mannosylation, and glycophospholipid anchor synthesis, and some of the pathology may derive from these defects, not explored here. Furthermore, little is known about the glycosylation-independent functions of dolichol, considered as a general membrane component in mammalian cells (Rip et al., 1985).

The pathogenesis and phenotypic specificity of CDGs deserves further investigations. However, our results point to an unsuspected role for a steroid reductase-like enzyme in the pathogenesis of one type of CDG, presumably mediated by a requirement for dolichol synthesis.

EXPERIMENTAL PROCEDURES

Genome Mapping

All patients were enrolled according to approved human subjects protocol at respective institutions. DNA was extracted from peripheral blood leukocytes by salt extraction, genotyped with the Illumina Linkage IVb mapping panel (Murray et al., 2004), and analyzed with easyLINKAGE-Plus software (Hoffmann and Lindner, 2005). Parameters were set to autosomal recessive with full penetrance and disease allele frequency of 0.001. Genomic regions with LOD scores over 2 were considered as candidate intervals. Linkage simulations were performed with Allegro 1.2c under the same parameters, with 5000 markers at average 0.64 cM intervals, codominant allele frequencies, and parametric calculations (Hoffmann and Lindner, 2005).

Mutation and CDG Screening

We performed direct bidirectional sequencing of the five coding exons and splice junction sites of *SRD5A3* via BigDye Terminator cycle sequencing (Applied Biosystems). We screened 31 patients with CDG-Ix and seven patients from a cohort with CDG-Ix and either strong clinical overlap such as severe congenital eye malformation and/or indications for a dolichol-phosphate biosynthesis defect. Clinical description of patients 08-0486, 08-0487, and 07-0419 was previously reported, corresponding respectively to patients 3, 5, and 7 (Morava et al., 2008) and 25, 26, and 27 (Morava et al., 2009). CDG was diagnosed by affinity chromatography and mass-spectrometry analysis of transferrin (O'Brien et al., 2007) or with transferrin isoelectric focusing (de Jong et al., 1994).

GlcNAc-Transferase Assays in Fibroblasts

Skin fibroblasts from the patients and controls were cultured in Dulbecco's modified Eagle's medium 10% fetal calf serum. Microsomal membranes were prepared as described (Thiel et al., 2002) and suspended in 20 mM Tris-HCl (pH 7.1), 10 mM MgCl2, and 1 mM dithiothreitol (DTT).

Assay I

For measurement of the transfer of GlcNAc from UDP-GlcNAc to endogenous lipid acceptor in microsomal membranes, the reaction contained 50 mM Tris-HCl (pH 7.5), 0.1 μCi UDP-[^{14}C]GlcNAc (specific activity 262 mCi/ mmol),

(B) Mass spectra of Dolichol-15,16 in WT and *dfg10-100* yeast strains showing accumulation of corresponding polyprenols in the mutant strain. Single, double, and triple arrows highlight natural isotopic distribution, each offset by one atomic mass unit (amu). Polyprenol was detected only in mutant (red), by identification of a spectrum that partially overlapped with dolichol. Quantification of the dolichol content of yeast mutant indicates 70% reduction (after subtraction of polyprenol isotopic contribution; see the Experimental Procedures; white bar, WT; gray bar, mutant).

(C) Scans of Dolichol-18,19 in WT and E11.5 *Srd5a3*$^{Gt/Gt}$ embryos showing the accumulation of corresponding polyprenols in the mutant embryos.

(D) Ratio of polyprenol-18,19,20 to dolichol-18,19,20 calculated with lipid plasma level from control and *SRD5A3* mutated patients, showing a significant increase of these ratios compared to controls (n = 10) and other types of CDG (n = 4). Error bars represent the mean ± standard deviation. Two-tailed student's t test was used for statistical analysis. Color bars represent individual measurement for five patients with *SRD5A3* mutation. Error bar was not generated for pol-20/dol-20 ratio in the group CDGI-a,c as polyprenol levels were undetectable in three out of four patients.

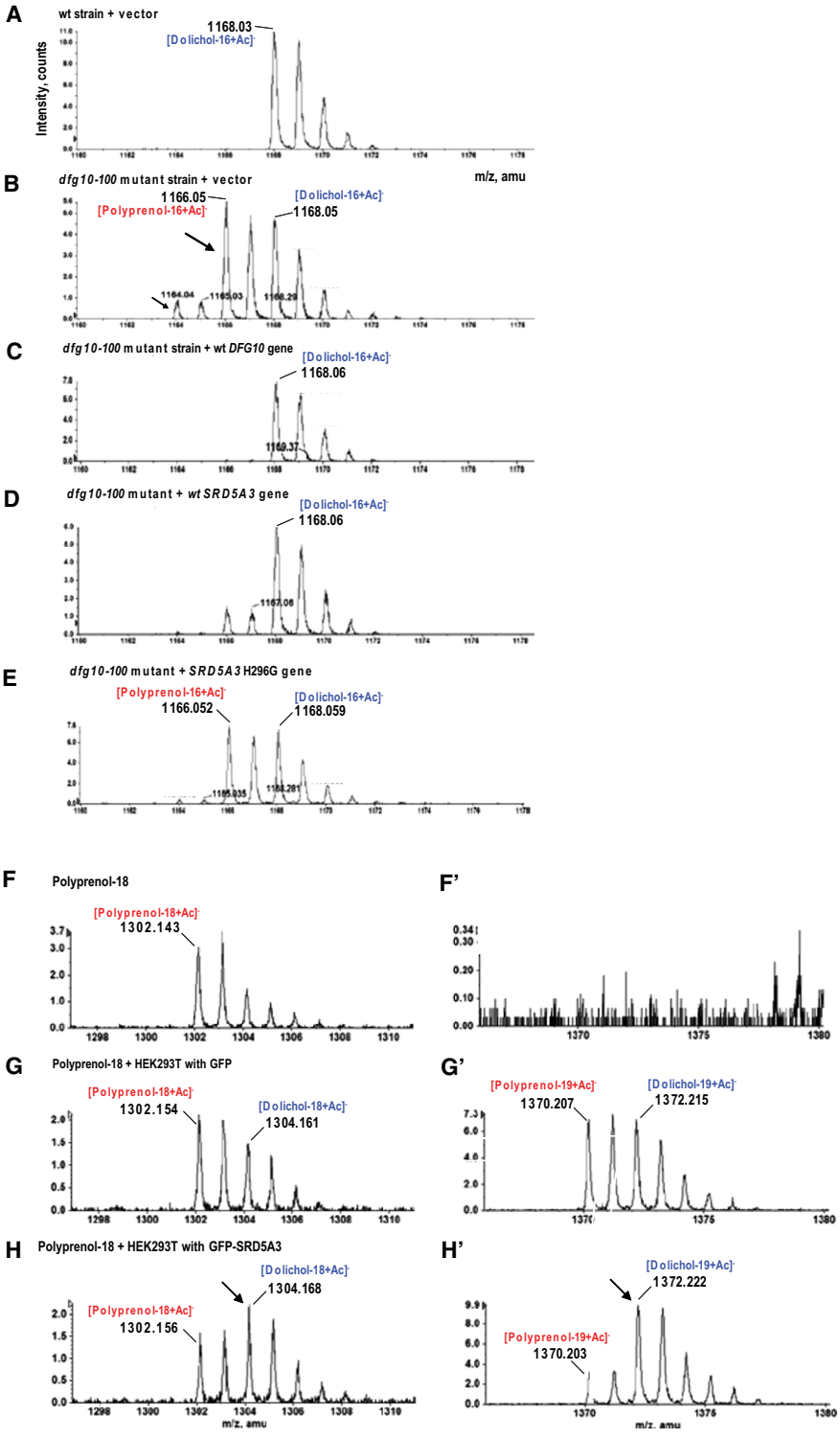

Figure 6. In Vivo and In Vitro Polyprenol Reduction Promoting Activity of SRD5A3

(A–E) LC-MS analysis of lipid extracts from yeast cultured in minimal media.

(A) Only dolichol is detected in WT yeast strains transformed with pYX212 empty vector.

(B) In *dfg10-100* strain transformed with pYX212 empty vector, accumulation of polyprenol relative to dolichol is evident. An additional compound (arrows) was tentatively identified as polyprenal, previously suggested as an intermediate in yeast during in vitro dolichol biosynthesis (Sagami et al., 1996).

(C) In the *dfg10-100* strain transformed with the WT *DFG10* gene, no polyprenol accumulation was detected.

15 mM MgCl2, 0.8 mM DTT, 26% glycerol, and 150 μg protein in a final volume of 60 μl. After 15 min at 24°C, the reaction was stopped with chloroform/methanol (3/2, by volume) and processed by phase partitioning (Sharma et al., 1982). Radioactive glycolipids were separated on silica gel 60 plates (Merck) developed in chloroform/methanol/water (65/25/4, by volume). Radioactivity was detected and quantified by phosphorimager (Molecular Dynamics).

Assay II

For determination of the transfer to exogenous Dol-P, the reaction contained 3.6 μg Dol-P, 2.4 mM diheptanoyl-phosphatidylcholine, 38 mM Tris-HCl (pH 7.5), 0.1 μCi UDP-[^{14}C]GlcNAc (specific activity 262 μCi/ mmol), 11 mM MgCl2, 0.7 mM DTT, 25% glycerol, and 150 μg protein in a final volume of 60 μl. Incubation and processing of the reaction was as in assay I.

Construction of DsRed-SRD5A3 and GFP-SRD5A3 Expression Plasmids

The ORF of *SRD5A3* was amplified from a human fetal brain complementary DNA (cDNA) library and cloned in phrGFP II-N (Stratagene) and pDsRed2-C1 (Clontech) vectors. Site-directed mutagenesis was performed with QuickChange II site-directed mutagenesis kit (Stratagene) according to the manufacturer's instructions.

Analysis of *Srd5a3* $^{Gt/Gt}$ Embryos, Microarray Experiments, and Quantitative PCRs

Frozen embryos (129/SvEvBrd × C57BL6/J mix) carrying a gene trap insertion in one allele of *Srd5a3* were obtained from Lexicon and transferred in pseudo-pregnant female (Renard and Babinet, 1984). Genotyping was performed by PCR with yolk sac-extracted DNA. Whole-transcriptome analysis was performed with the 44k Agilent genome oligo microarray kit with four embryos *Srd5a3*$^{Gt/Gt}$ and four littermate controls from two different litters. For these experiments, E8.5 embryos, which had not started the turning process and did not yet show morphological defect, were chosen. Real-time PCR reactions were performed in the LightCycler 480 system (Roche) with the SYBR Green I Master Kit (Roche). Seven of the eight genes found misregulated with the microarray experiment and tested by real-time PCR were found to be comparably and significantly misregulated. Animals were used in compliance with approved institutional policies.

Mass-Spectrometry Analysis of Yeast and Mouse Samples

Lipid extraction (Bligh and Dyer, 1959) and LC-MS analysis was performed as described (Garrett et al., 2007). For quantitative measurements, nor-dolichol (Avanti Polar Lipids) (Garrett et al., 2007) was added to the sample before lipid extraction. For a detailed description, please see the Extended Experimental Procedures.

Analysis of Plasma Polyprenoids

Plasma (500 μl) samples from controls (n = 10), all with normal transferrin isofocusing profile), CDG-I patients with known defect (n = 4), and SRD5A3 patients (n = 5) were subjected to saponification (Yasugi and Oshima, 1994) by addition of 5 M KOH in water (500 μl) and MeOH (1500 μl) for 1 hr at 100°C under nitrogen atmosphere. Lipids were extracted with hexane (2 × 1.5 ml), the organic phase was washed with 1.5 ml water, and dried. Samples were dissolved in hexane-MeOH (100 μl, 1:2 v/v), and 5 μl was injected on a 50 × 2 mm monolythic column (C18, Onyx) coupled to a Quattro LC-ESI tandem mass spectrometer (MicroMass). Polyprenoids were eluted with a MeOH/Isopropanol gradient containing 1% 50 mM LiI. MRM transitions [Dol-n]Li+ → 162+ and [Pren-n]Li+ → [Pren-n-H2O]Li+ were used to calculate response areas/ml plasma of respectively dolichols and polyprenols (n, number of isoprene units) (D'Alexandri et al., 2006).

Polyprenol Reduction Assay

The assay was performed as a modification of the procedure described previously (Sagami et al., 1993). The reaction mixture consisted of 50 mM Tris-HCl (pH 8.0), 1 mM DTT, 50 mM KF, 20% glycerol, 1 mM $MgCl_2$, 0.1% Triton X-100, and 4 μg/ml polyprenol C90, previously dissolved in ethanol. After 15 min sonication in a bath apparatus, the reaction was started with the addition of 5 mM NADPH and 700 μg crude cell-extract proteins, to a final volume of 250 μl. Reactions were incubated for 12 hr at 37°C. Samples were lipid extracted (Bligh and Dyer, 1959) after mixing with an internal standard of nor-dolichol and analyzed by LC-MS.

Bioinformatics

Phylogenetic tree representation was done with phylogeny (Dereeper et al., 2008). (http://www.phylogeny.fr/version2_cgi/index.cgi). Topology prediction was performed with TMHMM, a program for predicting membrane-spanning segments based on hidden Markov model (http://www.cbs.dtu.dk/services/TMHMM/). Pfam database was used to identify proteins with steroid 5α-reductase domain (PF02544) (http://pfam.sanger.ac.uk/family/PF02544/).

ACCESSION NUMBERS

Microarray data are available in the Array Express Archive database with accession number E-MEXP-2713 (http://www.ebi.ac.uk/microarray-as/ae/).

SUPPLEMENTAL INFORMATION

Supplemental Information includes Extended Experimental Procedures, six figures, and three tables and can be found with this article online at doi:10.1016/j.cell.2010.06.001.

ACKNOWLEDGMENTS

We thank G.R. Fink, A. Jansen, F. Karst, K. Gable, T.M. Dunn, and R. Kolodner for providing yeast strains and helpful advice. We are grateful to J.H. Lin for valuable discussion. We thank D. Matern and the Mayo Clinic for providing complete results of patients' transferrin analysis and also C. Sault for additional clinical results from family CVH-385. We thank the University of California, San Francisco, microscopy core (P30 NS047101 and DK80506) and the Biomedical Genomics Core for help in imaging and microarray data analysis. A. de Rooij and K. Huyben are gratefully acknowledged for technical assistance. H.H.F. is a Sanford Research Professor. He and B.N. are supported by the Rocket Fund, R01 DK55615, and the Sanford Children's Health Research Center. Financial support from Euroglycanet (LSHM-CT2005-512131) to R.W. and Metakids and the Netherlands Brain Foundation to D.L. are kindly acknowledged. L.L. was supported by grants from the Deutsche Forschungsgemeinschaft and the Körber-Stiftung. The mass-spectrometry facility in the Department of Biochemistry of the Duke University Medical Center and Z.G. are supported by the LIPID MAPS Large Scale Collaborative Grant GM-069338 from the National Institutes of Health. V.C. is supported by a fellowship from Fondation pour la Recherche Médicale, and J.G.G. is an

(D) Transformation of the *dfg10-100* strain with the human *SRD5A3* gene corrects polyprenol accumulation, although low levels are still detected.
(E) Transformation of the *dfg10-100* strain with the human *SRD5A3* enzymatically null H296G mutation fails to correct the polyprenol accumulation.
(F–H) LC-MS analysis of a lipid extract from an in vitro experiment performed with the exogenous substrate, polyprenol-18, in which cell lysates were used as the source of enzyme.
(F and F′) Polyprenol-18 spectrum after incubation in the reaction buffer without cell lysate. No polyprenol-19 or any forms of dolichol are evident.
(G and G′) After incubation with HEK293T cell lysate transfected with GFP, part of polyprenol-18 is elongated in polyprenol-19 and 28% is reduced to the corresponding dolichol.
(H and H′) In the presence of lysate from cell overexpressing GFP-SRD5A3, 67% of the initial polyprenol is reduced to dolichol (arrows). Both cell lysates show similar elongation of polyprenols.
See also Figures S5 and S6.

Investigator of the Howard Hughes Medical Institute. L.A.-G. ascertained and phenotyped family CVH-385 and MR3 and proposed the collaboration to identify the defective gene. W.B.D. reviewed brain imaging and suggested CDG defects, and H.F. suggested SRD5A3 as the polyprenol reductase. D.S., A.P.D.B., and H.v.B. coordinated homozygosity mapping. J.L.S. identified the SRD5A3 mutation, and S.L.B. performed linkage analysis and initiated generation of the gene trap mouse line. E.M. performed CDG Ix phenotype assessment on the remaining patients. D.J.L. performed biochemical diagnosis, functional studies, and dolichol analysis. R.A.W. coordinated biochemical analysis and homozygosity mapping. L.L. suggested a defect in dolichol biosynthesis and performed dolichol rescue experiments. E.S. helped with dolichol standards. D.B.-V., M.A., P.B., and J.S.C. contributed patients. Mass-spectrometry analysis was performed by Z.G. under the guidance of C.R.H.R. B.G.N. performed lipid extraction and patient LLO analysis. S.H. and B.R.A. provided technical assistance, discussions, and control samples. H.H. provided assistance with standard yeast techniques. V.C. performed all other experiments. J.G.G. directed the project. V.C. and J.G.G. wrote the manuscript, with help from the other authors.

Received: January 30, 2010
Revised: March 26, 2010
Accepted: May 6, 2010
Published online: July 15, 2010

REFERENCES

Acosta-Serrano, A., O'Rear, J., Quellhorst, G., Lee, S.H., Hwa, K.Y., Krag, S.S., and Englund, P.T. (2004). Defects in the N-linked oligosaccharide biosynthetic pathway in a Trypanosoma brucei glycosylation mutant. Eukaryot. Cell *3*, 255–263.

Aebi, M., and Hennet, T. (2001). Congenital disorders of glycosylation: genetic model systems lead the way. Trends Cell Biol. *11*, 136–141.

Aggarwal, S., Thareja, S., Verma, A., Bhardwaj, T.R., and Kumar, M. (2010). An overview on 5alpha-reductase inhibitors. Steroids *75*, 109–153.

Al-Gazali, L., Hertecant, J., Algawi, K., El Teraifi, H., and Dattani, M. (2008). A new autosomal recessive syndrome of ocular colobomas, ichthyosis, brain malformations and endocrine abnormalities in an inbred Emirati family. Am. J. Med. Genet. A. *146*, 813–819.

Alber, T., and Kawasaki, G. (1982). Nucleotide sequence of the triose phosphate isomerase gene of Saccharomyces cerevisiae. J. Mol. Appl. Genet. *1*, 419–434.

Allen, C.M., Jr., Kalin, J.R., Sack, J., and Verizzo, D. (1978). CTP-dependent dolichol phosphorylation by mammalian cell homogenates. Biochemistry *17*, 5020–5026.

Andersson, S., Berman, D.M., Jenkins, E.P., and Russell, D.W. (1991). Deletion of steroid 5 alpha-reductase 2 gene in male pseudohermaphroditism. Nature *354*, 159–161.

Behrens, N.H., and Leloir, L.F. (1970). Dolichol monophosphate glucose: an intermediate in glucose transfer in liver. Proc. Natl. Acad. Sci. USA *66*, 153–159.

Bligh, E.G., and Dyer, W.J. (1959). A rapid method of total lipid extraction and purification. Can. J. Biochem. Physiol. *37*, 911–917.

Chavan, M., and Lennarz, W. (2006). The molecular basis of coupling of translocation and N-glycosylation. Trends Biochem. Sci. *31*, 17–20.

Chojnacki, T., and Dallner, G. (1988). The biological role of dolichol. Biochem. J. *251*, 1–9.

D'Alexandri, F.L., Gozzo, F.C., Eberlin, M.N., and Katzin, A.M. (2006). Electrospray ionization mass spectrometry analysis of polyisoprenoid alcohols via Li+ cationization. Anal. Biochem. *355*, 189–200.

de Jong, G., van Noort, W.L., and van Eijk, H.G. (1994). Optimized separation and quantitation of serum and cerebrospinal fluid transferrin subfractions defined by differences in iron saturation or glycan composition. Adv. Exp. Med. Biol. *356*, 51–59.

Dereeper, A., Guignon, V., Blanc, G., Audic, S., Buffet, S., Chevenet, F., Dufayard, J.F., Guindon, S., Lefort, V., Lescot, M., et al. (2008). Phylogeny.fr: robust phylogenetic analysis for the non-specialist. Nucleic Acids Res. *36*(Web Server issue), W465–W469.

Eklund, E.A., and Freeze, H.H. (2006). The congenital disorders of glycosylation: a multifaceted group of syndromes. NeuroRx *3*, 254–263.

Ekström, T.J., Chojnacki, T., and Dallner, G. (1984). Metabolic labeling of dolichol and dolichyl phosphate in isolate hepatocytes. J. Biol. Chem. *259*, 10460–10468.

Ekström, T.J., Chojnacki, T., and Dallner, G. (1987). The alpha-saturation and terminal events in dolichol biosynthesis. J. Biol. Chem. *262*, 4090–4097.

Freeze, H.H. (2006). Genetic defects in the human glycome. Nat. Rev. Genet. *7*, 537–551.

Garrett, T.A., Guan, Z., and Raetz, C.R. (2007). Analysis of ubiquinones, dolichols, and dolichol diphosphate-oligosaccharides by liquid chromatography-electrospray ionization-mass spectrometry. Methods Enzymol. *432*, 117–143.

Grünewald, S., and Matthijs, G. (2000). Congenital disorders of glycosylation (CDG): a rapidly expanding group of neurometabolic disorders. Neuropediatrics *31*, 57–59.

Haeuptle, M.A., and Hennet, T. (2009). Congenital disorders of glycosylation: an update on defects affecting the biosynthesis of dolichol-linked oligosaccharides. Hum. Mutat. *30*, 1628–1641.

Hasilik, A., and Tanner, W. (1978). Carbohydrate moiety of carboxypeptidase Y and perturbation of its biosynthesis. Eur. J. Biochem. *91*, 567–575.

Helenius, A., and Aebi, M. (2001). Intracellular functions of N-linked glycans. Science *291*, 2364–2369.

Heller, L., Orlean, P., and Adair, W.L., Jr. (1992). Saccharomyces cerevisiae sec59 cells are deficient in dolichol kinase activity. Proc. Natl. Acad. Sci. USA *89*, 7013–7016.

Hoffmann, K., and Lindner, T.H. (2005). easyLINKAGE-Plus—automated linkage analyses using large-scale SNP data. Bioinformatics *21*, 3565–3567.

Jaeken, J., and Matthijs, G. (2007). Congenital disorders of glycosylation: a rapidly expanding disease family. Annu. Rev. Genomics Hum. Genet. *8*, 261–278.

Jaeken, J., Hennet, T., Matthijs, G., and Freeze, H.H. (2009). CDG nomenclature: time for a change!. Biochim. Biophys. Acta *1792*, 825–826.

Jones, M.B., Rosenberg, J.N., Betenbaugh, M.J., and Krag, S.S. (2009). Structure and synthesis of polyisoprenoids used in N-glycosylation across the three domains of life. Biochim. Biophys. Acta *1790*, 485–494.

Kahrizi, K., Najmabadi, H., Kariminejad, R., Jamali, P., Malekpour, M., Garshasbi, M., Ropers, H.H., Kuss, A.W., and Tzschach, A. (2009). An autosomal recessive syndrome of severe mental retardation, cataract, coloboma and kyphosis maps to the pericentromeric region of chromosome 4. Eur. J. Hm. Genet. *17*, 125–128.

Kato, S., Tsuji, M., Nakanishi, Y., and Suzuki, S. (1980). Enzymatic dephosphorylation of dolichyl pyrophosphate—the bacitracin-sensitive, rate-limiting step for dolichyl mannosyl phosphate synthesis in rat liver microsomes. Biochem. Biophys. Res. Commun. *95*, 770–776.

Keller, R.K., Jehle, E., and Adair, W.L., Jr. (1982). The origin of dolichol in the liver of the rat. Determination of the dietary contribution. J. Biol. Chem. *257*, 8985–8989.

Kohlwein, S.D., Eder, S., Oh, C.S., Martin, C.E., Gable, K., Bacikova, D., and Dunn, T. (2001). Tsc13p is required for fatty acid elongation and localizes to a novel structure at the nuclear-vacuolar interface in Saccharomyces cerevisiae. Mol. Cell. Biol. *21*, 109–125.

Kranz, C., Jungeblut, C., Denecke, J., Erlekotte, A., Sohlbach, C., Debus, V., Kehl, H.G., Harms, E., Reith, A., Reichel, S., et al. (2007). A defect in dolichol phosphate biosynthesis causes a new inherited disorder with death in early infancy. Am. J. Hum. Genet. *80*, 433–440.

Lau, K.S., Partridge, E.A., Grigorian, A., Silvescu, C.I., Reinhold, V.N., Demetriou, M., and Dennis, J.W. (2007). Complex N-glycan number and

degree of branching cooperate to regulate cell proliferation and differentiation. Cell *129*, 123–134.

Mahendroo, M.S., and Russell, D.W. (1999). Male and female isoenzymes of steroid 5alpha-reductase. Rev. Reprod. *4*, 179–183.

Marek, K.W., Vijay, I.K., and Marth, J.D. (1999). A recessive deletion in the GlcNAc-1-phosphotransferase gene results in peri-implantation embryonic lethality. Glycobiology *9*, 1263–1271.

Morava, E., Wosik, H., Kárteszi, J., Guillard, M., Adamowicz, M., Sykut-Cegielska, J., Hadzsiev, K., Wevers, R.A., and Lefeber, D.J. (2008). Congenital disorder of glycosylation type Ix: review of clinical spectrum and diagnostic steps. J. Inherit. Metab. Dis. *31*, 450–456.

Morava, E., Wosik, H.N., Sykut-Cegielska, J., Adamowicz, M., Guillard, M., Wevers, R.A., Lefeber, D.J., and Cruysberg, J.R. (2009). Ophthalmological abnormalities in children with congenital disorders of glycosylation type I. Br. J. Ophthalmol. *93*, 350–354.

Mösch, H.U., and Fink, G.R. (1997). Dissection of filamentous growth by transposon mutagenesis in Saccharomyces cerevisiae. Genetics *145*, 671–684.

Murray, S.S., Oliphant, A., Shen, R., McBride, C., Steeke, R.J., Shannon, S.G., Rubano, T., Kermani, B.G., Fan, J.B., Chee, M.S., and Hansen, M.S. (2004). A highly informative SNP linkage panel for human genetic studies. Nat. Methods *1*, 113–117.

Nishikawa, A., and Mizuno, S. (2001). The efficiency of N-linked glycosylation of bovine DNase I depends on the Asn-Xaa-Ser/Thr sequence and the tissue of origin. Biochem. J. *355*, 245–248.

O'Brien, J.F., Lacey, J.M., and Bergen, H.R., 3rd. (2007). Detection of hypo-N-glycosylation using mass spectrometry of transferrin. Curr. Protoc. Hum. Genet., *Chapter 17*, Unit 17.4.

Renard, J.P., and Babinet, C. (1984). High survival of mouse embryos after rapid freezing and thawing inside plastic straws with 1-2 propanediol as cryoprotectant. J. Exp. Zool. *230*, 443–448.

Rip, J.W., Rupar, C.A., Ravi, K., and Carroll, K.K. (1985). Distribution, metabolism and function of dolichol and polyprenols. Prog. Lipid Res. *24*, 269–309.

Rosenwald, A.G., Stanley, P., McLachlan, K.R., and Krag, S.S. (1993). Mutants in dolichol synthesis: conversion of polyprenol to dolichol appears to be a rate-limiting step in dolichol synthesis. Glycobiology *3*, 481–488.

Rossignol, D.P., Scher, M., Waechter, C.J., and Lennarz, W.J. (1983). Metabolic interconversion of dolichol and dolichyl phosphate during development of the sea urchin embryo. J. Biol. Chem. *258*, 9122–9127.

Ruiz-Canada, C., Kelleher, D.J., and Gilmore, R. (2009). Cotranslational and posttranslational N-glycosylation of polypeptides by distinct mammalian OST isoforms. Cell *136*, 272–283.

Russell, D.W., and Wilson, J.D. (1994). Steroid 5 alpha-reductase: two genes/two enzymes. Annu. Rev. Biochem. *63*, 25–61.

Sagami, H., Kurisaki, A., and Ogura, K. (1993). Formation of dolichol from dehydrodolichol is catalyzed by NADPH-dependent reductase localized in microsomes of rat liver. J. Biol. Chem. *268*, 10109–10113.

Sagami, H., Igarashi, Y., Tateyama, S., Ogura, K., Roos, J., and Lennarz, W.J. (1996). Enzymatic formation of dehydrodolichal and dolichal, new products related to yeast dolichol biosynthesis. J. Biol. Chem. *271*, 9560–9566.

Sharma, C.B., Lehle, L., and Tanner, W. (1982). Solubilization and characterization of the initial enzymes of the dolichol pathway from yeast. Eur. J. Biochem. *126*, 319–325.

Sidbury, R., and Paller, A.S. (2001). What syndrome is this? CHIME syndrome. Pediatr. Dermatol. *18*, 252–254.

Swiezewska, E., and Danikiewicz, W. (2005). Polyisoprenoids: structure, biosynthesis and function. Prog. Lipid Res. *44*, 235–258.

Thiel, C., Schwarz, M., Hasilik, M., Grieben, U., Hanefeld, F., Lehle, L., von Figura, K., and Körner, C. (2002). Deficiency of dolichyl-P-Man:Man7GlcNAc2-PP-dolichyl mannosyltransferase causes congenital disorder of glycosylation type Ig. Biochem. J. *367*, 195–201.

Uemura, M., Tamura, K., Chung, S., Honma, S., Okuyama, A., Nakamura, Y., and Nakagawa, H. (2008). Novel 5 alpha-steroid reductase (SRD5A3, type-3) is overexpressed in hormone-refractory prostate cancer. Cancer Sci. *99*, 81–86.

Vermeer, S., Kremer, H.P., Leijten, Q.H., Scheffer, H., Matthijs, G., Wevers, R.A., Knoers, N.A., Morava, E., and Lefeber, D.J. (2007). Cerebellar ataxia and congenital disorder of glycosylation Ia (CDG-Ia) with normal routine CDG screening. J. Neurol. *254*, 1356–1358.

Vleugels, W., Haeuptle, M.A., Ng, B.G., Michalski, J.C., Battini, R., Dionisi-Vici, C., Ludman, M.D., Jaeken, J., Foulquier, F., Freeze, H.H., et al. (2009). RFT1 deficiency in three novel CDG patients. Hum. Mutat. *30*, 1428–1434.

Wigley, W.C., Prihoda, J.S., Mowszowicz, I., Mendonca, B.B., New, M.I., Wilson, J.D., and Russell, D.W. (1994). Natural mutagenesis study of the human steroid 5 alpha-reductase 2 isozyme. Biochemistry *33*, 1265–1270.

Wolf, M.J., Rush, J.S., and Waechter, C.J. (1991). Golgi-enriched membrane fractions from rat brain and liver contain long-chain polyisoprenyl pyrophosphate phosphatase activity. Glycobiology *1*, 405–410.

Yasugi, E., and Oshima, M. (1994). Sequential microanalyses of free dolichol, dolichyl fatty acid ester and dolichyl phosphate levels in human serum. Biochim. Biophys. Acta *1211*, 107–113.